

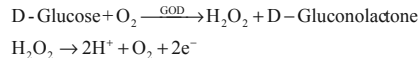
2.3 A 3 μ W Wirelessly Powered CMOS Glucose Sensor for an Active Contact Lens

Yu-Te Liao, Huanfen Yao, Babak Parviz, Brian Otis

University of Washington, Seattle, WA

The increase in the diabetes population makes glucose monitoring a pressing demand for clinical and continuous use. Non-invasive sensing would allow a painless, convenient solution compared to traditional skin-piercing glucose meters. Among various body fluids, tear fluid, which is correlated to the glucose concentration in blood [1], is directly accessible on the eye and can provide a unique opportunity to develop an interface between a sensor and the human body. The current technique is to collect tear fluid samples in capillary tubes and assay the samples for glucose *ex situ* using standard laboratory instrumentation. Integrating sensors into a contact lens would provide a way to continuously and reliably sense metabolites in tear fluids.

We present an integrated wirelessly powered glucose sensor allowing a functional active system on a contact lens. This sensor IC consists of power management, readout circuitry, wireless communication interface, and energy-storage capacitors in a standard CMOS process with no external components. Fig. 2.3.1 shows the electrochemical glucose sensor generating a current proportional to the glucose concentration. The main principles are as follows:



Amperometric results of a continuous flow test for low concentrations of glucose in tear film are shown. The sensor is composed of the working electrode (WE), counter electrode (CE) and reference electrode (RE). Using thin-film microfabrication techniques, the sensor is fabricated with 3 metal layers (Ti(10nm)/Pd(10nm)/Pt(100nm)) on a transparent polyethylene terephthalate (PET) polymer, and then molded to a lens shape with a diameter of 1cm, as shown in Fig. 2.3.1. The sensing area is 0.22mm². Glucose oxidase (GOD) and titanium isopropoxide are used to create a GOD/titania sol-gel membrane on the sensor area, which creates a measured sensitivity of 1.67 μ Amm⁻²mM⁻¹.

Our previous work demonstrated the potential value of integrating silicon chips, antenna, and an LED on a contact lens [2]. The basic functional elements required are energy delivery, sensing signal readout circuitry, signal processing, and communication subsystems. Each of these blocks must be designed for minimum energy consumption. An on-eye sensor would clearly not allow an on-board power source or battery, so power must be delivered wirelessly using far-field electromagnetic radiation or near-field inductive coupling. Near-field coupling requires a large inductance/transformer, making integration difficult in size-constrained applications. By considering the path loss, antenna efficiency and regulations on maximum RF power exposure to the human eye, we adopt a 2.4GHz carrier frequency for power delivery and data communication.

Another design challenge is the size of chip, which is limited to approximately 0.5 \times 0.5mm² due to the radius of curvature of the human eye. All active and passive components must be integrated into this area. Figure 2.3.2 shows the sensor readout architecture. A 3-stage full-wave rectifier is used to convert the incoming 2.4GHz RF power to a DC voltage supply, which is subsequently filtered by an on-chip 800pF capacitor. Since fluctuations in incident RF power cause supply variations, on-chip regulation is necessary. A sub- μ W low-power regulator and bandgap reference [3] provide a stable supply for the sensing electronics. We use a separate digital and analog supply-regulation technique [4] to reduce the noise coupling into the sensing element from the oscillator and logic switching noise. To provide isolation from digital and analog supply without adding an extra regulator, the regulator pass transistor is separated. This topology achieves 30dB isolation between digital and analog supplies. Figure 2.3.2 shows the low-power regulator schematic and the measured on-chip regulation with different input power levels. The minimum input power of the chip is 0dBm since the chip impedance is directly matched to the antenna without an external matching network.

Figure 2.3.3 shows the current readout circuitry. This readout circuitry includes a potentiostat, providing a stable 400mV voltage difference between the working and reference electrodes. The sensing current is injected into an oscillator-based current-to-frequency converter. The ring oscillator nominally operates at 250kHz, consumes 300nA, and is sensitive to additional injected current. The linear readout current range is 750nA. The bandgap voltage reference and a sub-threshold voltage divider [5] provide excellent stability to environmental variations. The measured frequency stability over 6 hours is shown in Fig. 2.3.3, showing a maximum frequency deviation less than 1kHz. The temperature variation is compensated to first-order through differential measurement of a reference oscillator and the sensing oscillator. Frequency-modulated load shifting key (FM-LSK) is used to transmit the sensing data to the reader. The backscattered signal encodes the glucose concentration as an offset-modulated frequency.

To measure the performance of the glucose sensor, we connect the molded sensor with the readout IC and then use a syringe pump to control a volume of test solution flowing through the sensor. A buffer solution (pH 7.4), consistent with physiological conditions, is added after each concentration to flush the remaining ions of the previous solution. The glucose level in tear-film is reported in the range of 0.1 to 0.6mM. Figure 2.3.4 shows the measured oscillator frequency change with different glucose concentrations from 0 to 2mM. The linear correlation coefficient is 0.9968 from 25 tested samples. Figure 2.3.5 shows the measured backscattered signal from the chip. The glucose concentration of 0.25mM results in a 450kHz frequency deviation of the backscattering carrier. The glucose sensor system consumes 3 μ W and can be powered over 15cm from an effective isotropically radiated power (EIRP) of 0.1W power source at 2.4GHz. The efficiency of the glucose sensor system is limited to the size of antenna, storage capacitance, and matching network. The frequency deviation of the backscattered carrier can be demodulated by a conventional FM receiver. Figure 2.3.6 is a performance summary of our CMOS glucose sensor system and Fig. 2.3.7 shows the micrograph of the chip. The small chip area, high level of integration, and low power of our system allows application in multiple bio-sensing tasks, including smart contact lenses.

Acknowledgments:

We would like to thank Dr. Ilkka Lahdesmaki, Jagdish Pandey, and Andy Lingley for helpful discussion in sensor design as well as the National Science Foundation for support.

References:

- [1] J.T. Baca, C.R. Taormina, E. Feingold, D.N. Finogold, J.J. Grabowski, S.A. Asher, "Mass spectral determination of fasting tear glucose concentrations in nondiabetic volunteers," *Clin. Chem.* vol. 53, pp. 1370-1372, 2007.
- [2] J. Pandey, Y.-T. Liao, A. Lingley, Babak Parviz, B. Otis, "Toward an active contact lens: integration of a wireless power harvesting IC," *IEEE Biomedical Circuits and Systems Conf.*, pp. 125-128, Nov. 2009.
- [3] D. Yeager, F. Zhang, A. Zarrasvand, and B. Otis, "A 9.2 μ A gen 2 compatible UHF RFID sensing tag with -12dBm sensitivity and 1.25 μ Vrms input-referred noise floor," *IEEE ISSCC Dig. Tech. Papers*, Feb. 2010.
- [4] M.M. Ahmadi, G. Jullien, "A wireless-implantable microsystem for continuous blood glucose monitoring," *IEEE Trans. on Biomedical Circuits and Systems*, vol. 3, pp. 169-179, June 2009.
- [5] K. N. Leung, P.K.T. Mok, "A sub-1-V 15ppm/ $^{\circ}$ C CMOS bandgap voltage reference without requiring low threshold voltage device," *IEEE J. Solid-State Circuits*, vol. 37, pp. 526-530, Apr. 2002.

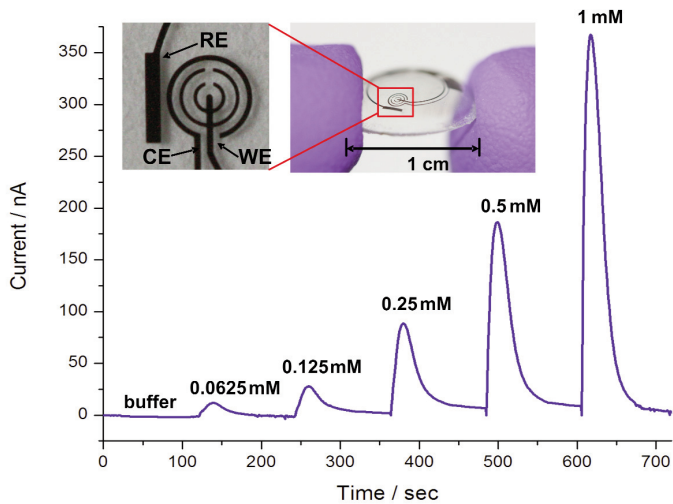


Figure 2.3.1: Photograph of assembled glucose sensor on a plastic substrate. The plot shows continuous glucose response measurements.

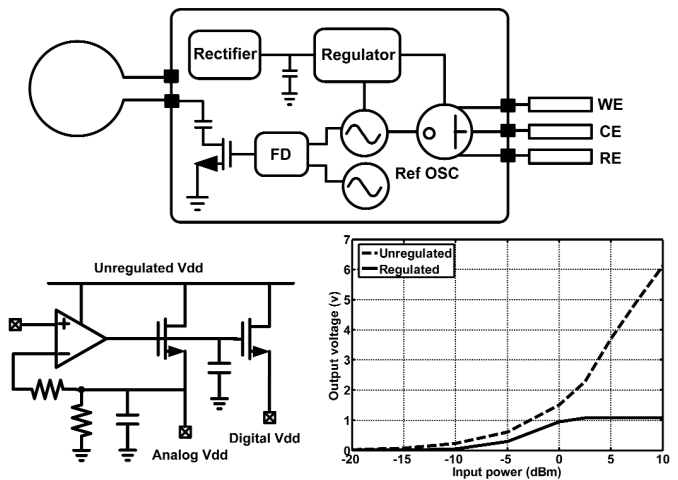


Figure 2.3.2: Block diagram of the wireless glucose sensor readout architecture and measured on-chip regulation.

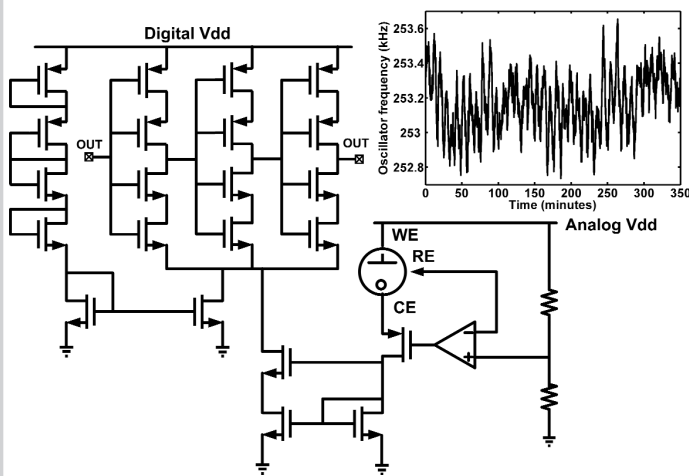


Figure 2.3.3: Current-sensing readout circuitry and measured frequency drifts.

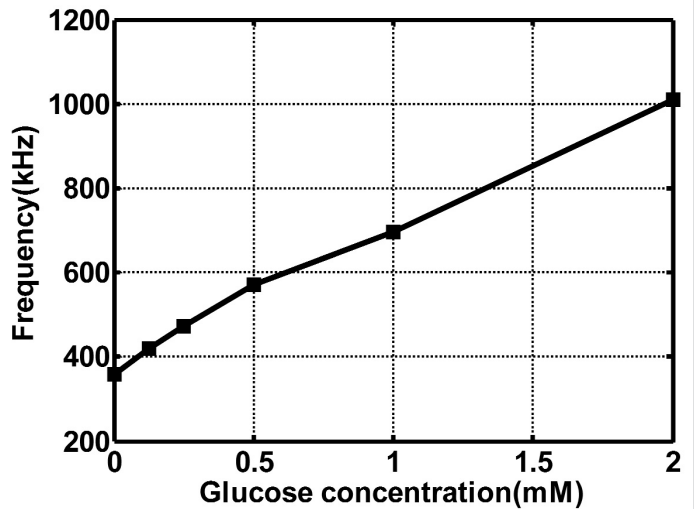


Figure 2.3.4: Measured oscillator output frequency vs. glucose concentration.

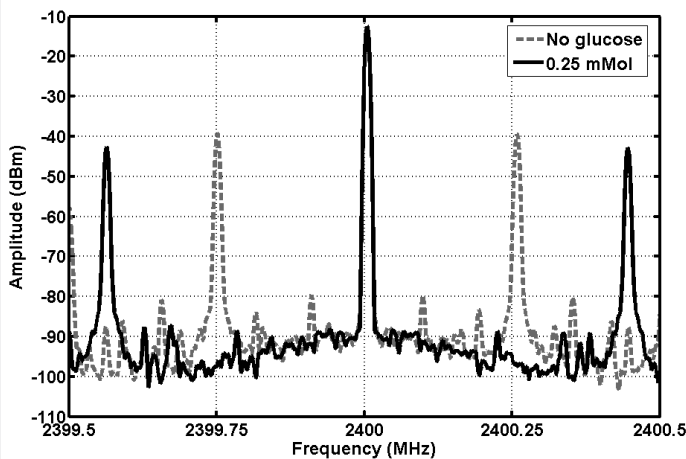


Figure 2.3.5: Measured wireless transmission results (backscattering).

	This work	[4]
Modulation scheme	LSK	LSK
Carrier frequency	2.4 GHz	13.56 MHz
Power consumption	3 μ W	110 μ W
Full scale measured current	750 nA	1 μ A
External component	No	Yes
Read range	15 cm (EIRP= 0.1W)	4 cm
Tempco (ppm) (35-45°C)	8300	N/A
Glucose detect range	0-2 mM (tear)	0-40 mM (blood)
Glucose sensitivity (μ Am ² mM ⁻¹)	1.67	N/A

Figure 2.3.6: Performance summary and comparison.

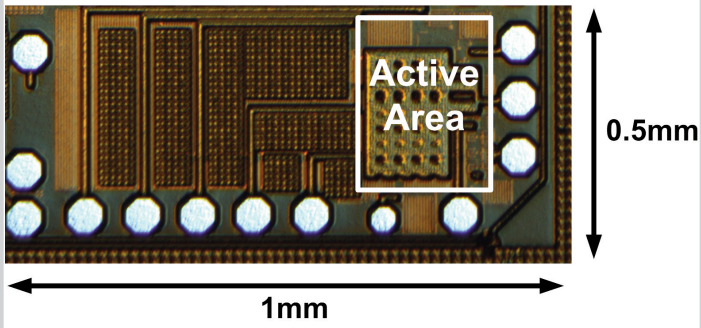


Figure 2.3.7: Die photograph.